Journal of Chromatography B, 879 (2011) 1987–1992

Contents lists available at ScienceDirect

Journal of Chromatography B

journal homepage: www.elsevier.com/locate/chromb

Short communication

Identification of hyperoside metabolites in rat using ultra performance liquid chromatography/quadrupole-time-of-flight mass spectrometry

Jianming Guo[1], Caifu Xue[1], Er-xin Shang, Jin-ao Duan*, Yuping Tang, Dawei Qian

Jiangsu Key Laboratory for TCM Formulae Research, Nanjing University of Chinese Medicine, Nanjing 210046, PR China

ARTICLE INFO

Article history:
Received 22 December 2010
Accepted 23 April 2011
Available online 6 May 2011

Keywords:
Hyperoside
UPLC/QTOFMS
Metabolynx

ABSTRACT

In this paper, ultra performance liquid chromatography (UPLC)/quadrupole-time-of-flight mass spectrometry (QTOF) with automated data analysis software (MetabolynxTM) were applied for fast analysis of hyperoside metabolites in rat after intravenous administration. MS^E was used for simultaneous acquisition of precursor ion information and fragment ion data at high and low collision energy in one analytical run, which facilitated the fast structural characterization of 12 metabolites in rat plasma, urine and bile. The results indicated that methylation, sulfation and glucuronidation were the major metabolic pathways of hyperoside *in vivo*, and among them, 3′-*O*-methyl-hyperoside was confirmed by matching its fragmentation patterns with standard compound. The present study provided important information about the metabolism of hyperoside which will be helpful for fully understanding the mechanism of this compound's action. Furthermore, this work demonstrated the potential of the UPLC/QTOFMS approach using Metabolynx for fast and automated identification of metabolites of natural product.

1. Introduction

Hyperoside (quercetin 3-*O*-galactoside) (HYP) is one of the major components of *Hypericum perforatum* (St. John's wort) [1]. It was also detected in many plant species such as *Abelmoschus manihot* [2], Black Currant [3], *Rosa agrestis* [4], *Ligularia fischeri* [5–9]. Hyperoside was reported to have antioxidant effect [10–12], antidepressant-like effect [13], antiviral activity [14], antifungal activity [15]. Hyperoside could protect against cerebral ischemia–reperfusion injury [16,17] and present anti-inflammatory activity [18–20].

To fully understand the mechanism of hyperoside's action, it is important to study the metabolic profile of hyperoside *in vivo*. Although there were reports about the pharmacokinetic study of hyperoside in rat after intravenous administration [21], the metabolite profile of hyperoside has not yet been studied. Furthermore, Chang et al. [22] showed that when administered at 6.0 mg/kg p.o. hyperoside could not be detected in plasma of rats either as the unchanged form or as its aglycone or conjugated aglycone form. Observations from the *in vitro* Caco-2 monolayer model and in situ intestinal perfusion model indicated that hyperoside has quite limited permeability [23,24]. It is conceivable that hyperoside not detectable after oral administration was due to low oral bioavailability or ring degradations by microbial or enzyme transformation in gastrointestinal. Therefore, in our study, hyperoside was administered intravenously.

In this paper, ultra performance liquid chromatography/quadrupole time-of-flight mass spectrometry (UPLC/QTOFMS) with automated data analysis (MetabolynxTM) were used for fast analysis of metabolic profile of hyperoside after intravenous administration. This method, with minimal operator intervention, reduces data interpretation time and produces high-quality structural information efficiently.

2. Experimental

2.1. Chemicals and reagents

Hyperoside was purchased from the National Institute for the Control of Pharmaceutical and Biological Products (Beijing, China); its chemical structure is shown in Fig. 1. Isorhamnetin-3-*O*-galactopyranoside was purchased from Wuhu delta Medical Technology Company Inc. (Anhui, China). HPLC grade acetonitrile and water were obtained from TEDIA Company Inc. (Fairfield, USA). Formic acid was obtained from Merck KGaA (Darmstadt, Germany). Other reagents and chemicals were of analytical grade.

2.2. Preparation of hyperoside for intravenous injection

Hyperoside was dissolved in saline containing 5% Tween 80 and 5% ethanol to form a solution for intravenous administration with a concentration of 2 mg/mL.

* Corresponding author. Tel.: +86 25 85811116; fax: +86 25 85811116.
E-mail address: dja@njutcm.edu.cn (J.-a. Duan).
[1] Guo and Xue contributed equally to this work.

1570-0232/$ – see front matter © 2011 Elsevier B.V. All rights reserved.
doi:10.1016/j.jchromb.2011.04.031

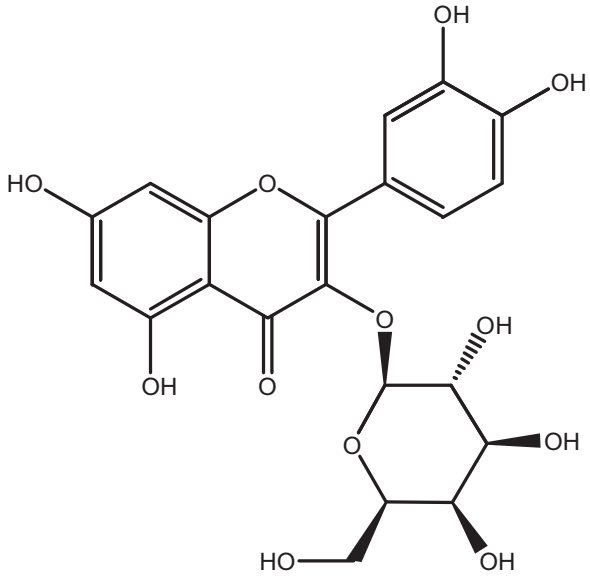

Fig. 1. Structure of hyperoside.

2.3. Animal experiments

Nine male Sprague-Dawley rats (200–250 g) obtained from Shanghai Slac Laboratory Animal Co. LTD (Shanghai) were used for plasma and urine collection. Animals were bred in a breeding room with temperature of 24 ± 2 °C, humidity of 60 ± 5%, and 12 h dark–light cycle. They were given tap water and fed normal food *ad libitum*. Animal welfare and experimental procedures were strictly in accordance with the *Guide for the Care and Use of Laboratory Animals* (US National Research Council, 1996) and the related ethics regulations of our University. Animal protocol was reviewed and approved by an internal animal care and use committee of Nanjing University of Chinese Medicine.

Whole blood samples (~0.5 mL) were collected in heparinized polythene tubes 5, 15, 30 and 60 min after intravenous administration of hyperoside (10 mg/kg), and immediately centrifuged at 1500 × *g* for 10 min at 4 °C to obtain plasma. Urine samples from three rats were collected during 0–12 h after the administration, respectively. Blank plasma and urine samples were collected before the administration of hyperoside. Rats were anesthetized by intraperitoneal administration of urethane (25%, w/v, 4 mL/kg) and applied with a cystic duct cannula operation. Bile samples were collected before and between 2 h after dosing. All samples were kept at −70 °C.

Rat plasma (100 μL) collected was mixed with 5 μL acetic acid and mixed for 10 s on a vortex-mixer. Then 5 mL ethyl acetate was added to 10 mL conical centrifuge tube and vortexed thoroughly for 3 min. After centrifugation for 10 min at 2000 × *g*, 4.0 mL organic phase in the upper layer were carefully transferred to another tube and evaporated to dryness under a stream of nitrogen at 40 °C. The residue was dissolved in 100 μL mobile phase and centrifuged at 12,000 × *g* for 10 min. For the analysis of urine and bile, the samples were mixed with acetonitrile and centrifuged at 12,000 × *g* for 10 min and 5 μL was used for analysis.

2.4. Ultra performance liquid chromatography–mass spectrometer (UPLC–MS)

Chromatography was performed on an ACQUITY UPLC system (Waters Corp., Milford, MA, USA) with a conditioned autosampler at 4 °C. The separation was carried out on an ACQUITY UPLC HSS T3 column (100 mm × 2.1 mm i.d., 1.8 μm; Waters Corp., Milford, MA, USA). The column temperature was maintained at 35 °C. The analysis was achieved with gradient elution using (A) acetonitrile and (B) water (containing 0.05% formic acid) as the mobile phase. The gradient condition was: 0–2 min 10% A; 2–6 min, linear from 12% to 17% A; 6–9 min, linear from 17% to 20% A; 9–12 min, linear from 20% to 80% A; held at 80% A for 2 min and then an immediate reduction to 10% A for equilibration of the column. The injection volume was 10 μL.

The Waters ACQUITY™ Synapt Mass Spectrometer (Waters Corp., Manchester, UK) was connected to the UPLC system via an electrospray ionization (ESI) interface. The ESI source was operated in negative ionization mode with the capillary voltage at 3.0 kV. The temperature of the source and desolvation was set at 120 °C and 350 °C, respectively. The cone and desolvation gas flows were 50 L h^{-1} and 600 L h^{-1}, respectively. All data collected in Centroid mode were acquired using Masslynx™ NT4.1 software (Waters Corp., Milford, MA, USA).

Leucine-enkephalin was used as the lock mass generating an $[M-H]^-$ ion (*m*/*z* 554.2615) at a concentration of 200 pg/mL and flow rate of 100 μL/min to ensure accuracy during the MS analysis. An MSE experiment was carried out as follows: Function 1: 6 V collision energy; function 2: collision energy ramp of 15–40 V. MSE enables almost simultaneous acquisition of both LC/MS and fragmentation data from a single experiment.

2.5. Data analysis

Post-acquisition analyses were performed using a Metabolynx™ (v4.1) program (Waters Corp., Milford, MA, USA), which employs an extensive list of potential biotransformation reactions (e.g. hydroxylation, methylation), in combination with the elemental compositions of the substrate molecules, to generate a series of extracted ion chromatograms (XICs). These XICs are compared between the control and sample to eliminate those chromatographic peaks in the sample that also appear in the control.

3. Results and discussion

3.1. Separation and identification of metabolites

The UPLC-MS profiles obtained from rat plasma, urine and bile revealed a complex pattern of metabolites (Fig. 2a–c). Using negative ion electrospray tandem mass spectrometry, parent compound hyperoside and 12 metabolites (Table 1) were detected in rat plasma, urine and bile compared with blank samples, which were hyperoside conjugates with glucuronyl, methyl, or sulfate groups. With careful setting of key parameters of Metabolynx, this method is able to show the presence of multi-type metabolites with only a limited requirement for manual intervention. Our results indicated that methylation, sulfation and glucuronidation were the major metabolic pathways of hyperoside *in vivo*.

3.2. Classes of metabolites identified using Metabolynx™

3.2.1. Parent compound (M1)

Hyperoside was detected in rat plasma and urine based on the same retention time and MS spectra of authentic standard (Figs. 2a,b and 3).

3.2.2. Methylated metabolites (M4 and M5)

In the rat plasma, M5 with *m*/*z* 477 (retention time 9.77 min, Supplementary Fig. 1a) was 14 Da (CH2) higher than the protonated ion of hyperoside, indicating that it was methylated hyperoside. Based on the same retention time and MS spectra with standard,

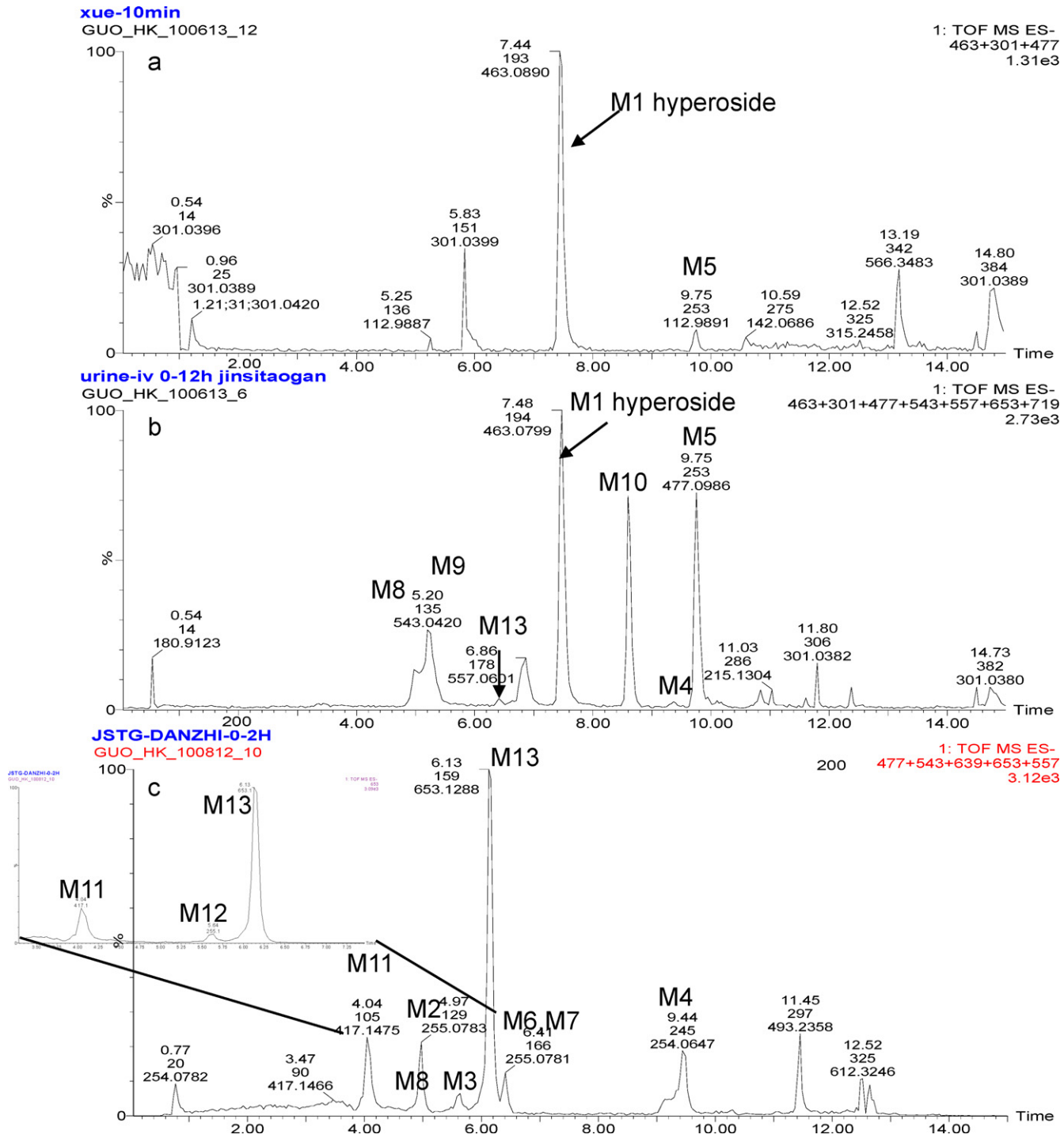

Fig. 2. UPLC/MS chromatograms of rat plasma, urine and bile sample after i.v. administration of hyperoside: (a) plasma sample, (b) urine sample, and (c) bile sample. Metabolite numbers in rat plasma, urine and bile samples are labeled. Selected ion monitoring (SIM) mode was used to show the existence of metabolites. Data are representative for three independent experiments.

the structure of M5 could be unambiguously identified as 3′-*O*-methylated hyperoside.

In rat urine, besides M5, there was another peak (M4) with *m*/*z* 477 (retention time 9.37 min), which was suspected to be the methylated metabolite, but the amount was lower than 3′-*O*-methyl-hyperoside. The enzyme responsible for methylation *in vivo* was catechol-*O*-methyltransferase (COMT), which is an intracellular enzyme widely distributed throughout the mammalian organs, and is able to methylate only one of the two neighbor catechol hydroxyls [25]. Thus COMT is presumed to be involved in the transformation, and it favors 3-*O*-methylation over 4-*O*-methylation [26]. Based on the above statement, M4 was tentatively identified as 4′-*O*-methyl-hyperoside.

The above methylated hyperoside metabolites (M4 and M5) were also detected in rat bile.

3.2.3. *Monoglucuronides metabolites (M2, M3, M11, M12 and M13)*

Diagnostic losses corresponding to glucuronide conjugates ($C_6H_8O_6$ 176 Da) were observed in the mass spectra of M2, M3 (*m*/*z*

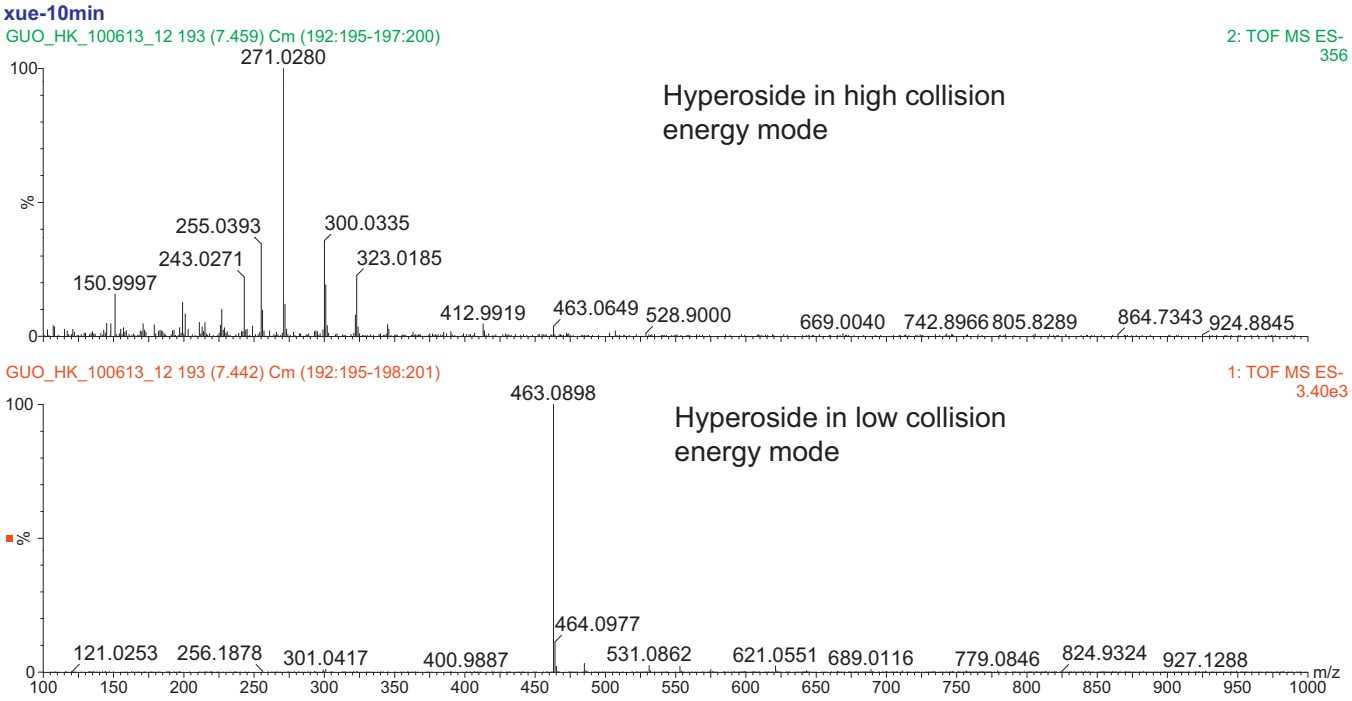

Fig. 3. TOFMS spectra of hyperoside (m/z 463) with MSE function at low and high energy.

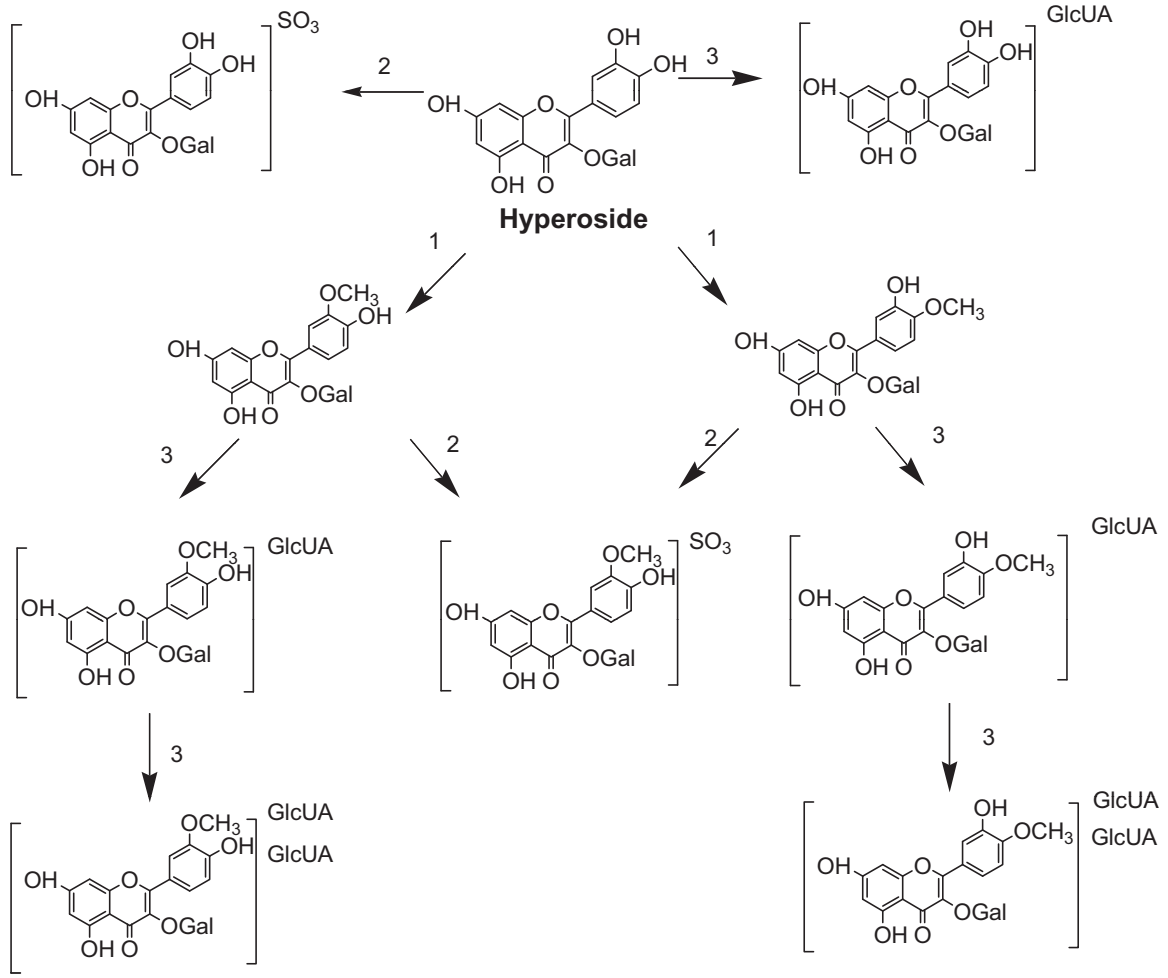

Fig. 4. Structures of hyperoside and its major metabolites and possible biotransformation pathways: 1: methylation; 2: sulfation; 3: glucuronidation.

Table 1
UPLC/ESI-MS, retention time (RT) and fragment ions of hyperoside and its metabolites in rat.

No.	RT (min)	*m/z* Calculate	*m/z* Found	Identification	Formula	Error (ppm)	Source[a]
M1	7.46	464.0955	463.0898	Parent	$C_{21}H_{20}O_{12}$	4.5	U, P
M2	4.97	640.1276	639.1199	Hyperoside monoglucuronide	$C_{27}H_{28}O_{18}$	0.3	B
M3	5.52	640.1276	639.1156	Hyperoside monoglucuronide	$C_{27}H_{28}O_{18}$	−6.4	B
M4	9.43	477.1033	477.1044	4′-*O*-methyl-hyperoside	$C_{22}H_{22}O_{12}$	2.3	U, B
M5	9.77	477.1033	477.1040	3′-*O*-methyl-hyperoside	$C_{22}H_{22}O_{12}$	1.5	U, P, B
M6	6.75	557.0601	557.0612	Methylated hyperoside sulfate	$C_{22}H_{22}O_{15}S$	2.0	U, B
M7	6.37	557.0601	557.0608	Methylated hyperoside sulfate	$C_{22}H_{22}O_{15}S$	1.3	U, B
M8	5.01	543.0445	543.0461	Hyperoside sulfate	$C_{21}H_{20}O_{15}S$	2.9	U, B
M9	5.25	543.0445	543.0433	Hyperoside sulfate	$C_{21}H_{20}O_{15}S$	−2.2	U
M10	8.60	720.0844	719.3627	Hyperoside sulfate monoglucuronide	$C_{27}H_{28}O_{21}S$		U
M11	4.04	654.1225	653.1356	Methylated hyperoside monoglucuronide	$C_{28}H_{30}O_{18}$	0.3	B
M12	5.64	654.1225	653.1334	Methylated hyperoside monoglucuronide	$C_{28}H_{30}O_{18}$	−2.0	B
M13	6.13	654.1225	653.1339	Methylated hyperoside monoglucuronide	$C_{28}H_{30}O_{18}$	−2.3	U, B

[a] U represents the urine samples, B the bile samples, and P the plasma samples.

639, Supplementary Fig. 1b). M2 and M3 were 176 Da higher than the protonated ion of hyperoside, therefore, M2, M3 were identified as hyperoside glucuronide.

M11, M12 and M13 (*m/z* 653, Supplementary Fig. 1c) were 14 Da (CH2) higher than the protonated ion of M2 and M3, indicating that they were methylated hyperoside glucuronide.

In rat urine, one metabolite was identified as glucuronide conjugates of methyl-hyperoside (Fig. 2b). In rat bile, two metabolites were identified as glucuronide conjugates of hyperoside and three metabolites as glucuronide conjugates of methyl-hyperoside (Fig. 2c). Their different retention times indicated different positionings of the methyl and/or glucuronide groups on hyperoside molecule, changing the polarity and the elution behavior of these molecules.

No glucuronide conjugate of hyperoside was detected in rat plasma.

3.2.4. Sulfates metabolites (M6, M7, M8 and M9)

Diagnostic lost corresponding to sulfate conjugates (SO_3 80 Da) were observed in the mass spectra of M8 and M9 (*m/z* 543 Supplementary Fig. 1d) in rat urine. M8 and M9 were 80 Da higher than the protonated ion of hyperoside and were identified as hyperoside metabolites contained a sulfate moiety (Table 1). M6 and M7 (*m/z* 557 Supplementary Fig. 1e) were 14 Da (CH2) higher than the protonated ion of M8 and M9, indicating that it was methylated hyperoside sulfate.

M6, M7, M8 and M9 were identified in rat urine (Fig. 2b). In rat bile, M6, M7 and M8 were identified (Fig. 2c).

3.2.5. Monoglucuronide sulfate metabolites (M10)

M10 was 256 Da higher than the protonated ion of hyperoside. Diagnostic loss of 256 Da was corresponding to glucuronide conjugates ($C_6H_8O_6$ 176 Da) and sulfate conjugates (SO_3 80 Da), therefore, M10 was identified as monoglucuronide sulfate metabolites of hyperoside and presented in rat urine (Fig. 2b).

There are a large number of components in the biofluids, among which many compounds may elute in the same time with the target compounds during analysis. In order to solve this problem, during the initial part of analysis for urine and plasma, the gradient elution with a mobile phase containing less organic solvent was used to yield early elution of the polar compounds in biofluid samples, which leads to the separation of endogenous components from the target compounds. This approach might also be useful in minimizing ion suppression from co-elutions.

Moreover, when post-acquisition analyses were performed using a Metabolynx, peaks present in the analyte were evaluated relative to the control samples by comparing their retention time, MS spectra and peak area. When a peak was included as metabolite, the peak area in the analyte had to be at least 5 times greater than that of the control.

4. Conclusion

In this paper, we described a method using ultra performance liquid chromatography/quadrupole time-of-flight mass spectrometry (UPLC/QTOFMS) with automated data analysis (MetabolynxTM) for fast analysis of metabolic profile of hyperoside in rat plasma, urine and bile after intravenous administration. It provides unique high throughput capabilities for drug metabolism study, with excellent MS accuracy and enhanced MS^E data acquisition. With MS^E technique, both molecular mass and fragment ion information can be generated in a way that provides similar information to conventional MS^2.

A total of 12 metabolites and parent compound hyperoside were identified in plasma, urine and bile compared with blank samples. With careful setting of key parameters, this method is able to show the presence of a wide range of metabolites with only a limited requirement for manual intervention and data interpretation time. Our results indicated that methylation, sulfation and glucuronidation were the major metabolic pathways of hyperoside *in vivo* (Fig. 4).

It is better to isolate the conjugated metabolites from urine and to determine their structures using NMR spectroscopy, while because of the low amounts of metabolites in urine it is hard to isolate these metabolites. And although there was report about the synthesis of quercetin glucuronides and sulfates, these glucuronide and sulfate metabolites were unstable [27].

In our study, a possible metabolism pathway on the biotransformation of hyperoside is established. It is worthwhile to further study the pharmacokinetics and tissue distribution of hyperoside and its major metabolites. And the software used in our study could not identify active versus non-active metabolites. Whether the newly identified methylated, glucuronide and sulfate metabolites of hyperoside are bioactive remains to be tested.

Acknowledgements

This work was supported by National Natural Science Foundation of China (No. 30902006), Jiangsu Provincial TCM Administration Bureau Project (No. LZ09011), 2009' Program for Excellent Scientific and Technological Innovation Team of Jiangsu Higher Education and 2009 Program for New Century Excellent Talents by the Ministry of Education (NCET-09-0163), Construction Project for Jiangsu Key Laboratory for High Technology Research of TCM Formulae (BM2010576), Construction Project for Jiangsu Engineering Center of Innovative Drug from Blood-conditioning TCM

Formulae. We are also pleased to thank Waters China for technical support.

Appendix A. Supplementary data

Supplementary data associated with this article can be found, in the online version, at doi:10.1016/j.jchromb.2011.04.031.

References

[1] Y. Wei, Q. Xie, W. Dong, Y. Ito, J. Chromatogr. A 1216 (2009) 4313.
[2] J. Guo, E.X. Shang, J.A. Duan, Y. Tang, D. Qian, S. Su, Rapid Commun. Mass Spectrom. 24 (2010) 443.
[3] D. He, Y. Huang, A. Ayupbek, D. Gu, Y. Yang, H.A. Aisa, Y. Ito, J. Liq. Chromatogr. Relat. Technol. 33 (2010) 615.
[4] L. Bitis, S. Kultur, G. Melikoglu, N. Ozsoy, A. Can, Nat. Prod. Res. 24 (2010) 580.
[5] A. Millet, F. Stintzing, I. Merfort, J. Pharm. Biomed. Anal. 53 (2010) 137.
[6] X. Yang, X. Zhang, Z. Yuan, X. Li, L. Zhang, L. Fan, J. Chromatogr. Sci. 47 (2009) 714.
[7] X.L. Piao, X.Y. Mi, Y.Z. Tian, Q. Wu, H.S. Piao, Z. Zeng, D. Wang, X. Piao, Arch. Pharm. Res. 32 (2009) 1689.
[8] J. Lee, D.S. Jang, N.H. Yoo, Y.M. Lee, J.H. Kim, J.S. Kim, J. Sep. Sci. 33 (2010) 582.
[9] Y. Cui, Q. Wang, X. Shi, X. Zhang, X. Sheng, L. Zhang, Phytochem. Anal. 21 (2010) 253.
[10] M.J. Piao, K.A. Kang, R. Zhang, D.O. Ko, Z.H. Wang, H.J. You, H.S. Kim, J.S. Kim, S.S. Kang, J.W. Hyun, Biochim. Biophys. Acta 1780 (2008) 1448.
[11] H.B. Li, X. Yi, J.M. Gao, X.X. Ying, H.Q. Guan, J.C. Li, Pharmacology 82 (2008) 105.
[12] Z. Liu, X. Tao, C. Zhang, Y. Lu, D. Wei, Biomed. Pharmacother. 59 (2005) 481.
[13] J. Schulte Haas, E. Dischkaln Stolz, A. Heemann Betti, A.C. Stein, J. Schripsema, G.L. Poser, S.M. Kuze Rates, Planta Med. (2010).
[14] L.L. Wu, X.B. Yang, Z.M. Huang, H.Z. Liu, G.X. Wu, Acta Pharmacol. Sin. 28 (2007) 404.
[15] S. Li, Z. Zhang, A. Cain, B. Wang, M. Long, J. Taylor, J. Agric. Food Chem. 53 (2005) 32.
[16] H.Y. Chen, J.H. Wang, Z.X. Ren, X.B. Yang, Zhong Xi Yi Jie He Xue Bao 4 (2006) 526.
[17] Z. Chen, C. Ma, W. Zhao, Yao Xue Xue Bao 33 (1998) 14.
[18] S. Lee, H.S. Park, Y. Notsu, H.S. Ban, Y.P. Kim, K. Ishihara, N. Hirasawa, S.H. Jung, Y.S. Lee, S.S. Lim, E.H. Park, K.H. Shin, T. Seyama, J. Hong, K. Ohuchi, Phytother. Res. 22 (2008) 1552.
[19] S. Sosa, R. Pace, A. Bornancin, P. Morazzoni, A. Riva, A. Tubaro, R. Della Loggia, J. Pharm. Pharmacol. 59 (2007) 703.
[20] S. Lee, S.H. Jung, Y.S. Lee, M. Yamada, B.K. Kim, K. Ohuchi, K.H. Shin, Arch. Pharm. Res. 27 (2004) 628.
[21] X. Liu, D. Wang, S.Y. Wang, X.S. Meng, W.J. Zhang, X.X. Ying, T.G. Kang, Yakugaku Zasshi 130 (2010) 873.
[22] Q. Chang, Z. Zuo, M.S. Chow, W.K. Ho, Eur. J. Pharm. Biopharm. 59 (2005) 549.
[23] Z. Zuo, L. Zhang, L. Zhou, Q. Chang, M. Chow, Life Sci. 79 (2006) 2455.
[24] G. Juergenliemk, K. Boje, S. Huewel, C. Lohmann, H.J. Galla, A. Nahrstedt, Planta Med. 69 (2003) 1013.
[25] P.T. Mannisto, S. Kaakkola, Pharmacol. Rev. 51 (1999) 593.
[26] J. Guo, F. Qian, J. Li, Q. Xu, T. Chen, Clin. Chem. 53 (2007) 465.
[27] P.W. Needs, P.A. Kroon, Tetrahedron 62 (2006) 6862.